

MA 11.1: Imaging topological defects in a non-collinear antiferromagnet

Aurore Finco

Laboratoire Charles Coulomb
Team Solid-State Quantum Technologies (S2QT)

CNRS and Université de Montpellier, Montpellier, France



DPG SKM 2023, March 27th 2023, Dresden

slides available at <https://magimag.eu>

Acknowledgments

L2C, Montpellier

Angela Haykal, Pawan Kumar, Vincent Jacques

UMR CNRS/Thales, Palaiseau

Pauline Dufour, Vincent Garcia, Stéphane Fusil

SPEC, CEA Gif-sur-Yvette

Anne Forget, Dorothée Colson, Jean-Yves Chauleau, Michel Viret

Synchrotron Soleil

Nicolas Jaouen



European Research Council

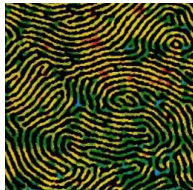
Established by the European Commission



Universal patterns in lamellar systems

Block copolymer

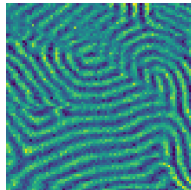
Period 40 nm



T. A. Witten. *Phys. Today* 43 (1990), 21

BiFeO₃ magnetic cycloid

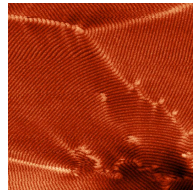
Period 64 nm



A. Finco et al. *Phys. Rev. Lett.* 128 (2022), 187201

FeGe magnetic helix

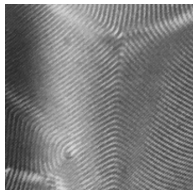
Period 70 nm



P. Schönherr et al. *Nat. Phys.* 14 (2018), 465

Liquid crystals

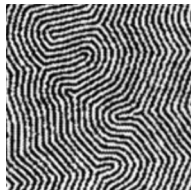
Period 800 nm



Y. Bouligand. *Dislocations in solids* (1983), Chap. 23

Ferrimagnetic garnet

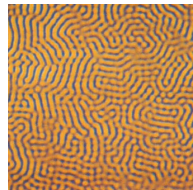
Period 8 μm



M. Seul et al. *Phys. Rev. A* 46 (1992), 7519

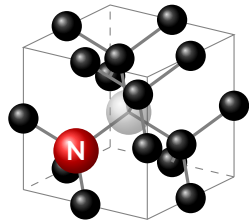
Fluid diffusion

Period 250 μm



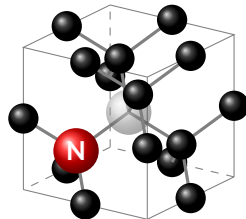
Q. Ouyang et al. *Chaos* 1 (1991), 411

NV centers for magnetic imaging



Defect in diamond

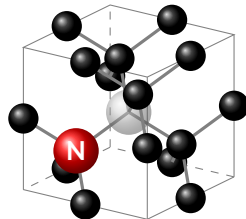
NV centers for magnetic imaging



Defect in diamond

- Optical manipulation and reading
- Ambient conditions

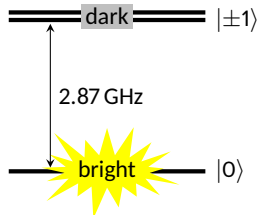
NV centers for magnetic imaging



Defect in diamond

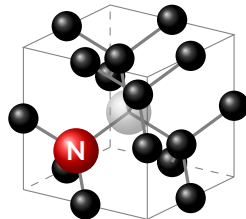
- Optical manipulation and reading
- Ambient conditions

Spin-dependent
fluorescence



NV ground state
spin $S = 1$

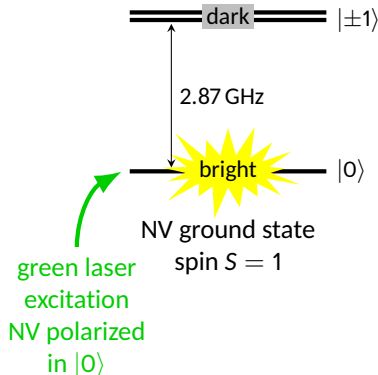
NV centers for magnetic imaging



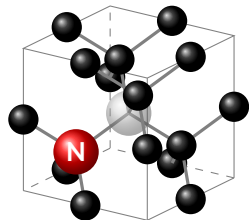
Defect in diamond

- Optical manipulation and reading
- Ambient conditions

Spin-dependent fluorescence

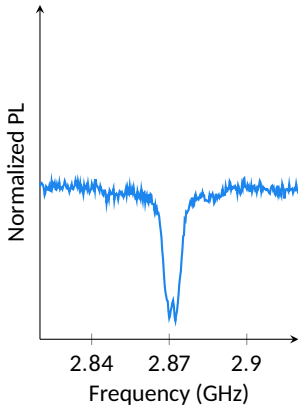
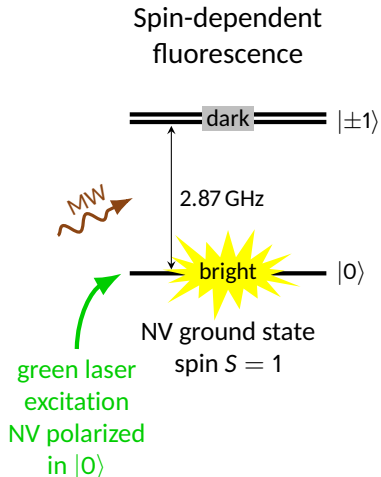


NV centers for magnetic imaging

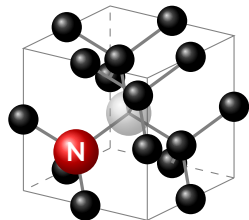


Defect in diamond

- Optical manipulation and reading
- Ambient conditions

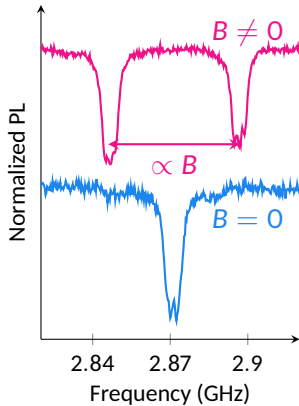
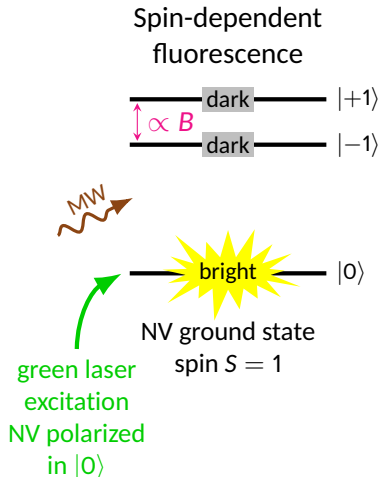


NV centers for magnetic imaging

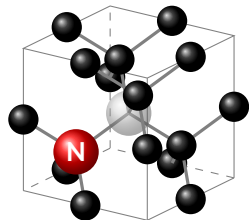


Defect in diamond

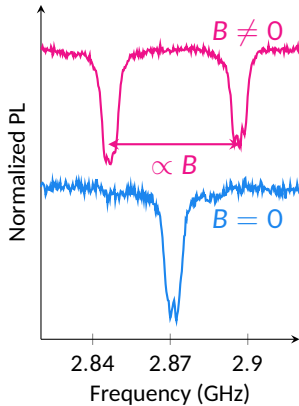
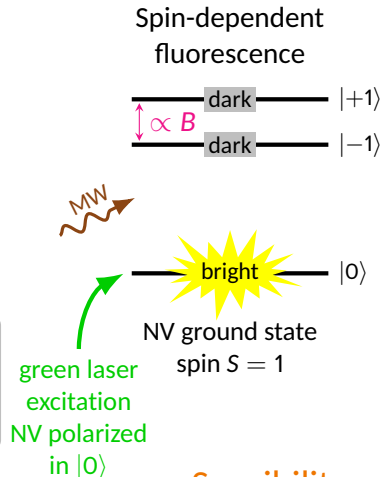
- Optical manipulation and reading
- Ambient conditions



NV centers for magnetic imaging



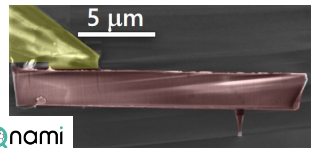
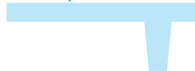
- Optical manipulation and reading
- Ambient conditions



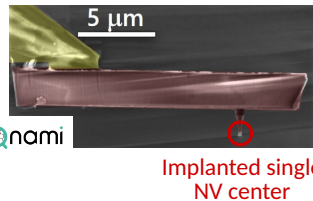
Sensibility: a few $\mu\text{T}/\sqrt{\text{Hz}}$

The scanning NV microscope setup

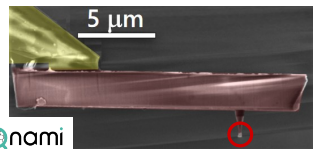
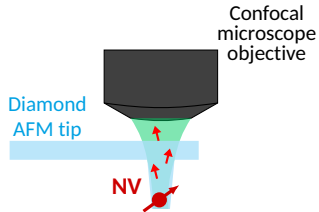
Diamond
AFM tip



The scanning NV microscope setup

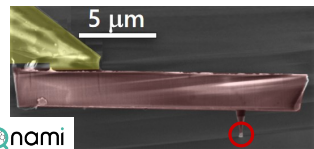
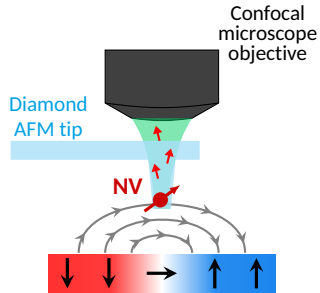


The scanning NV microscope setup



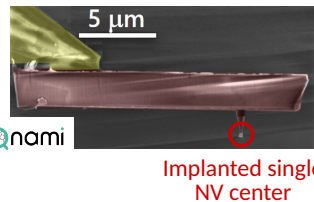
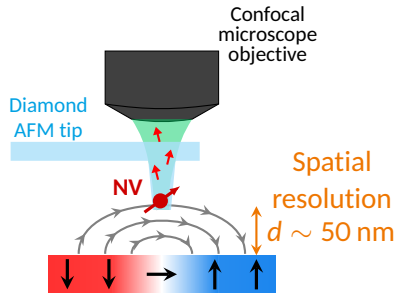
Implanted single
NV center

The scanning NV microscope setup



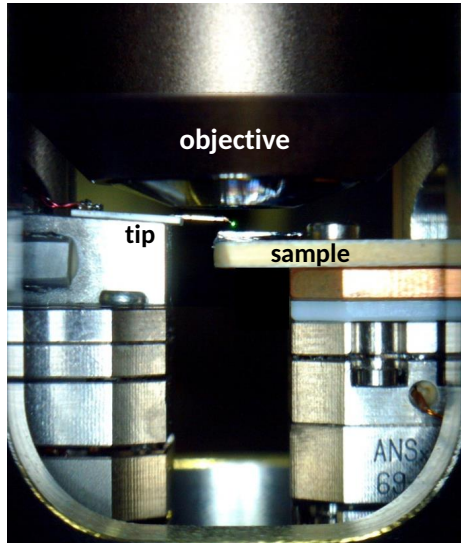
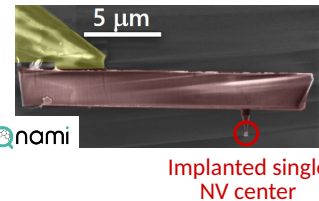
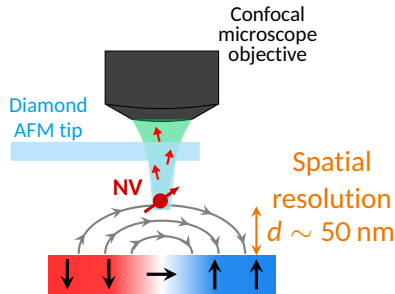
Implanted single
NV center

The scanning NV microscope setup



P. Maletinsky et al. *Nat. Nano.* 7 (2012), 320

The scanning NV microscope setup



Application to nanoscale magnetic texture imaging

Quantitative

Non-perturbative

Highly sensitive

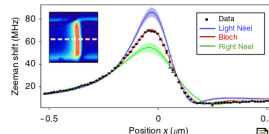
Application to nanoscale magnetic texture imaging

Determination of domain wall chirality

Quantitative

Non-perturbative

Highly sensitive



J.-P. Tetienne et al. *Nat Commun.* 6 (2015), 6733

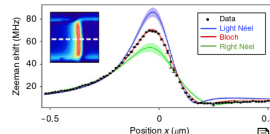
Application to nanoscale magnetic texture imaging

Quantitative

Non-perturbative

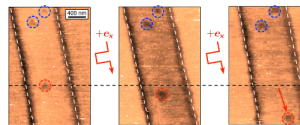
Highly sensitive

Determination of domain wall chirality



J.-P. Tetienne et al. *Nat Commun.* 6 (2015), 6733

Imaging of current-induced skyrmion movement



W. Akhtar et al. *Phys. Rev. Appl.* 11 (2019), 034066

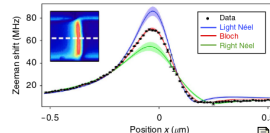
Application to nanoscale magnetic texture imaging

Quantitative

Non-perturbative

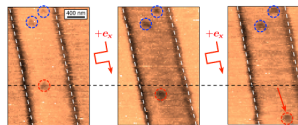
Highly sensitive

Determination of domain wall chirality



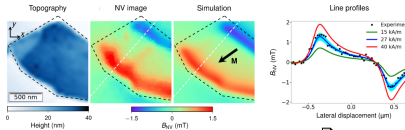
J.-P. Tetienne et al. *Nat Commun.* 6 (2015), 6733

Imaging of current-induced skyrmion movement



W. Akhtar et al. *Phys. Rev. Appl.* 11 (2019), 034066

Quantitative characterization of 2D ferromagnets

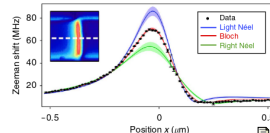


F. Fabre et al. *Phys. Rev. Mat.* 5 (2021), 034008

Application to nanoscale magnetic texture imaging

Quantitative

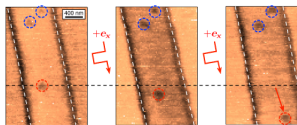
Determination of domain wall chirality



J.-P. Tetienne et al. *Nat Commun.* 6 (2015), 6733

Non-perturbative

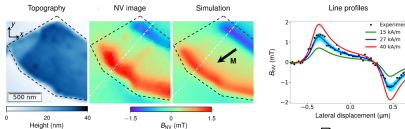
Imaging of current-induced skyrmion movement



W. Akhtar et al. *Phys. Rev. Appl.* 11 (2019), 034066

Highly sensitive

Quantitative characterization of 2D ferromagnets

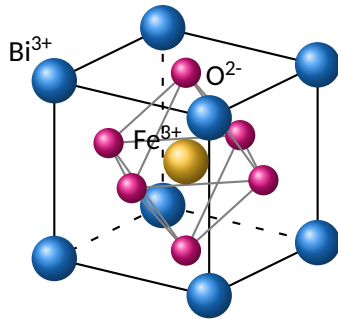


F. Fabre et al. *Phys. Rev. Mat.* 5 (2021), 034008

Great tool to
image antiferromagnets!

Bismuth ferrite, a room-temperature multiferroic

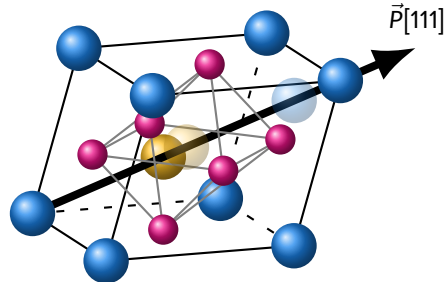
Electric polarization



Paraelectric phase ($T > 1100$ K)

Bismuth ferrite, a room-temperature multiferroic

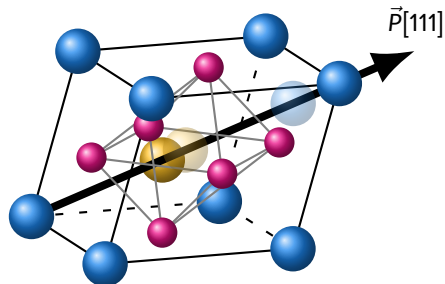
Electric polarization



Ferroelectric phase ($T < 1100$ K)

Bismuth ferrite, a room-temperature multiferroic

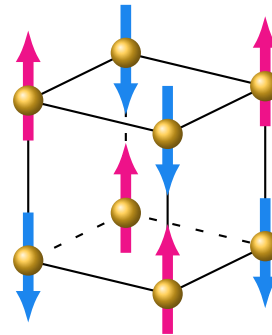
Electric polarization



Ferroelectric phase ($T < 1100$ K)

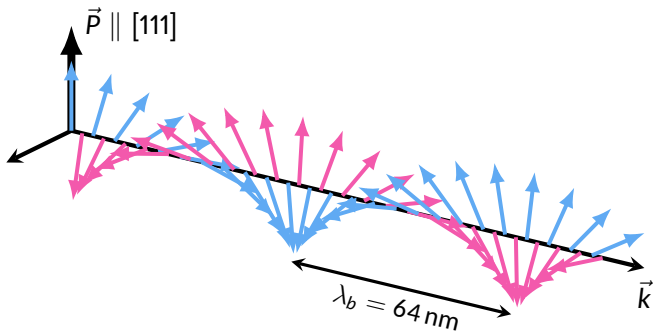
G. Catalan et al. *Adv. Mater.* 21 (2009), 2463–2485

Magnetism



G-type antiferromagnetic
phase ($T_N = 643$ K)

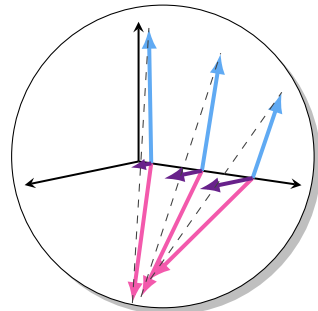
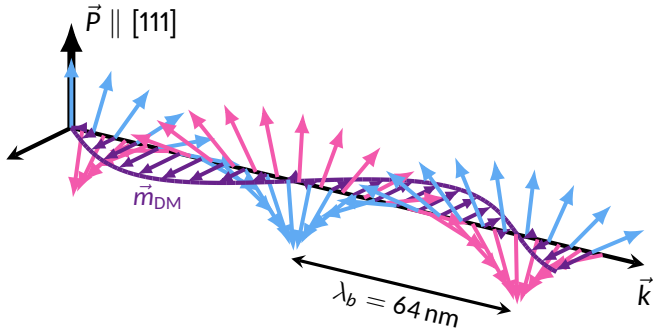
The effects of magnetoelectric coupling in BiFeO₃



Fully compensated cycloid

→ **No stray field!**

The effects of magnetoelectric coupling in BiFeO₃

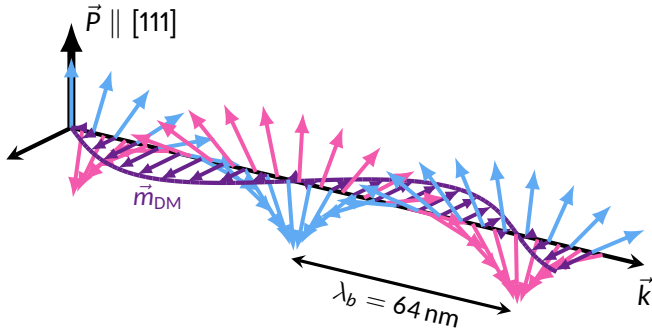


Spin density wave

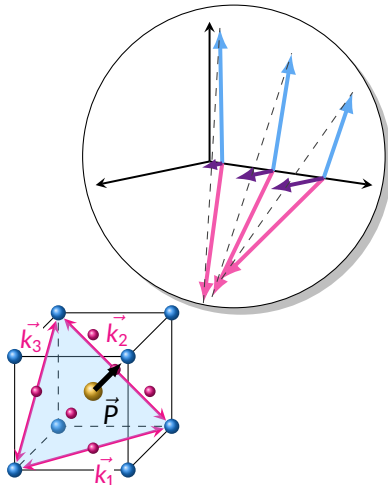
Weak uncompensated moment

→ Small stray field

The effects of magnetoelectric coupling in BiFeO₃



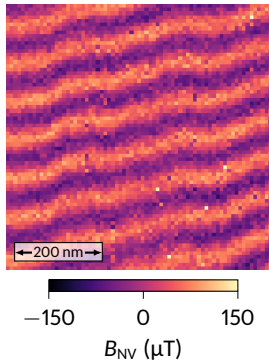
Spin density wave
Weak uncompensated moment
→ Small stray field



Quantitative analysis of the cycloid in bulk single crystal

Collaborations: UMR CNRS/Thales, Palaiseau (V. Garcia, S. Fusil)

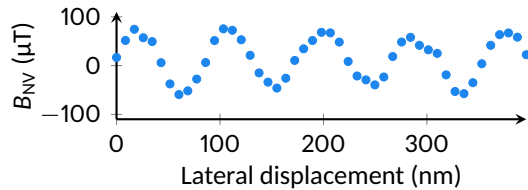
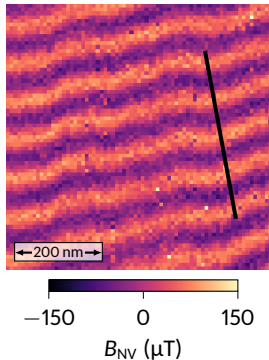
CEA SPEC, Gif-sur-Yvette (J.-Y. Chauleau, M. Viret)



Quantitative analysis of the cycloid in bulk single crystal

Collaborations: UMR CNRS/Thales, Palaiseau (V. Garcia, S. Fusil)

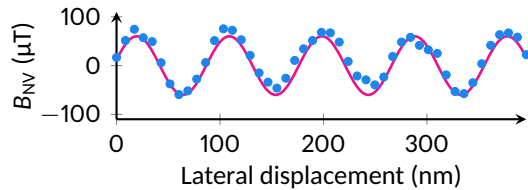
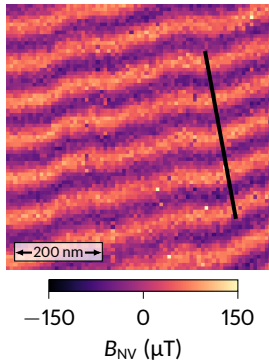
CEA SPEC, Gif-sur-Yvette (J.-Y. Chauleau, M. Viret)



Quantitative analysis of the cycloid in bulk single crystal

Collaborations: UMR CNRS/Thales, Palaiseau (V. Garcia, S. Fusil)

CEA SPEC, Gif-sur-Yvette (J.-Y. Chauleau, M. Viret)

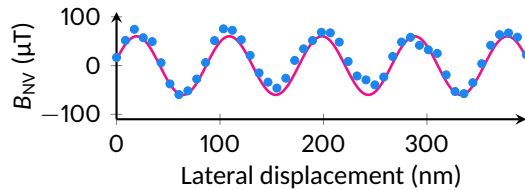
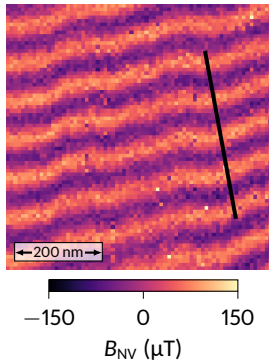


$$\begin{cases} B_x = 0 \\ B_y = -\frac{A}{\sqrt{2}} (\text{Re}\{S\} - \text{Im}\{S\}) \\ B_z = \sqrt{2} A \text{Re}\{S\} \end{cases} \quad \text{with} \quad \begin{cases} A = \frac{\mu_0 m_{\text{DM}}}{\sqrt{3} a^3} \sinh\left(\frac{ka}{2\sqrt{2}}\right) \\ S = e^{-kz/\sqrt{2}} e^{ik(y-z)/\sqrt{2}} \frac{1 - e^{-kt(1+i)/\sqrt{2}}}{1 - e^{-ka(1+i)/\sqrt{2}}} \end{cases}$$

Quantitative analysis of the cycloid in bulk single crystal

Collaborations: UMR CNRS/Thales, Palaiseau (V. Garcia, S. Fusil)

CEA SPEC, Gif-sur-Yvette (J.-Y. Chauleau, M. Viret)



$$m_{\text{DM}} = 0.09 \pm 0.03 \mu_B$$

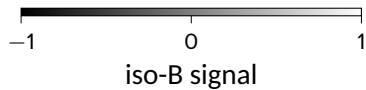
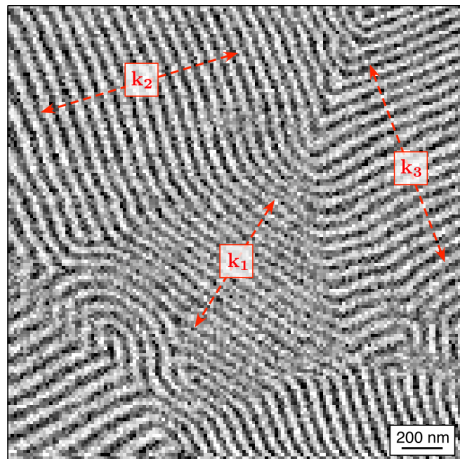
M. Ramazanoglu et al. *Phys. Rev. Lett.* 107 (2011), 207206

$$\begin{cases} B_x = 0 \\ B_y = -\frac{A}{\sqrt{2}} (\text{Re}\{S\} - \text{Im}\{S\}) \\ B_z = \sqrt{2} A \text{Re}\{S\} \end{cases}$$

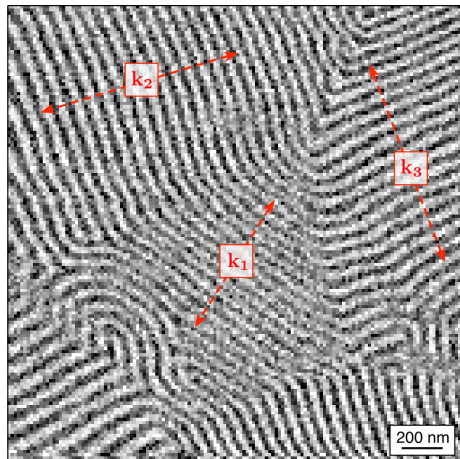
with

$$\begin{cases} A = \frac{\mu_0 m_{\text{DM}}}{\sqrt{3} a^3} \sinh\left(\frac{ka}{2\sqrt{2}}\right) \\ S = e^{-kz/\sqrt{2}} e^{ik(y-z)/\sqrt{2}} \frac{1 - e^{-kt(1+i)/\sqrt{2}}}{1 - e^{-ka(1+i)/\sqrt{2}}} \end{cases}$$

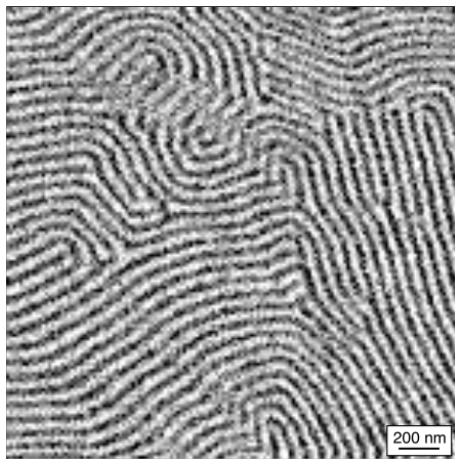
Rotation of the cycloid propagation direction measured in real space...



Rotation of the cycloid propagation direction measured in real space...



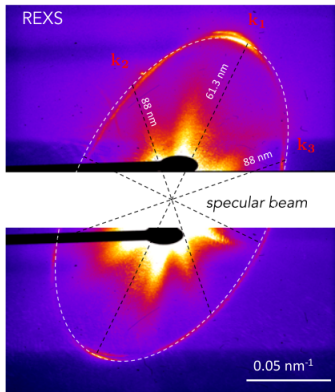
iso-B signal



iso-B signal

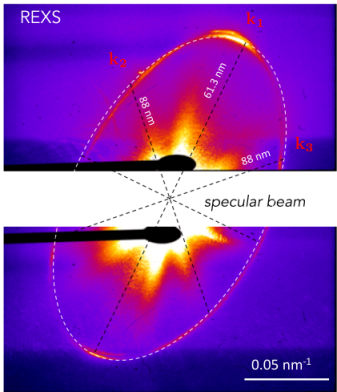
... and in reciprocal space

Resonant X-ray scattering

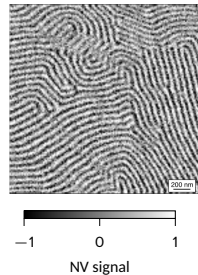
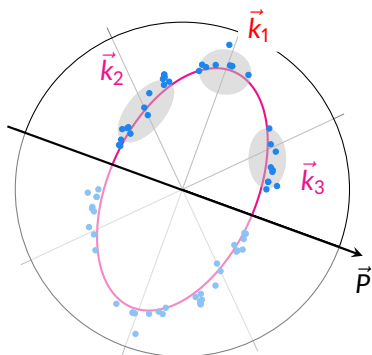


... and in reciprocal space

Resonant X-ray scattering



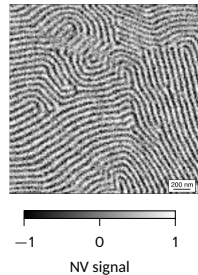
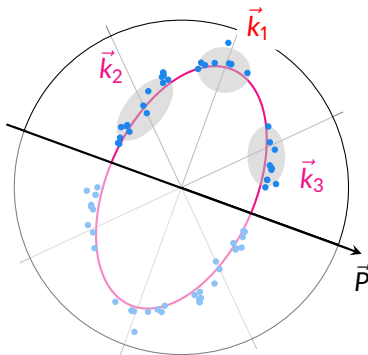
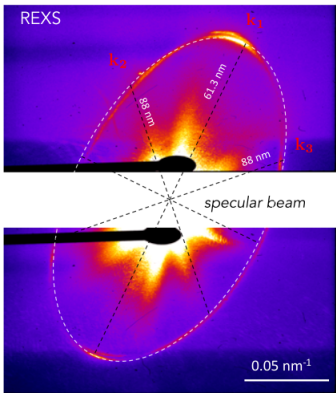
Polar plot of $\frac{2\pi}{\lambda}$ vs \vec{k} direction



... and in reciprocal space

Polar plot of $\frac{2\pi}{\lambda}$ vs \vec{k} direction

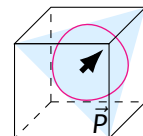
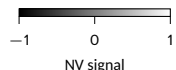
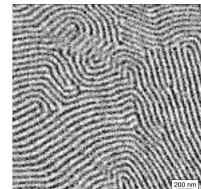
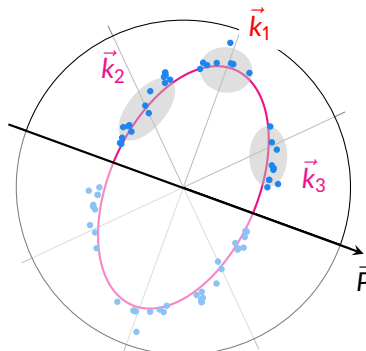
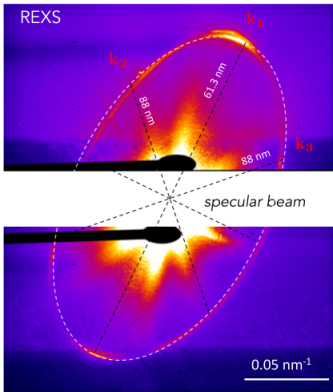
Resonant X-ray scattering



... and in reciprocal space

Polar plot of $\frac{2\pi}{\lambda}$ vs \vec{k} direction

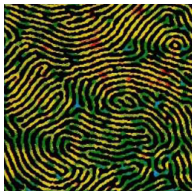
Resonant X-ray scattering



Universal patterns in lamellar systems

Block copolymer

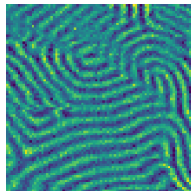
Period 40 nm



T. A. Witten. *Phys. Today* 43 (1990), 21

BiFeO₃ magnetic cycloid

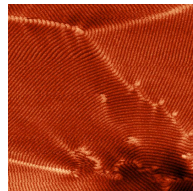
Period 64 nm



A. Finco et al. *Phys. Rev. Lett.* 128 (2022), 187201

FeGe magnetic helix

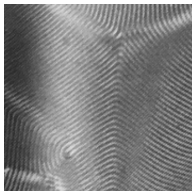
Period 70 nm



P. Schönherr et al. *Nat. Phys.* 14 (2018), 465

Liquid crystals

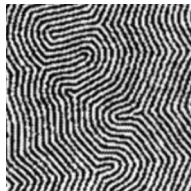
Period 800 nm



Y. Bouligand. *Dislocations in solids* (1983), Chap. 23

Ferrimagnetic garnet

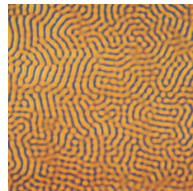
Period 8 μm



M. Seul et al. *Phys. Rev. A* 46 (1992), 7519

Fluid diffusion

Period 250 μm



Q. Ouyang et al. *Chaos* 1 (1991), 411

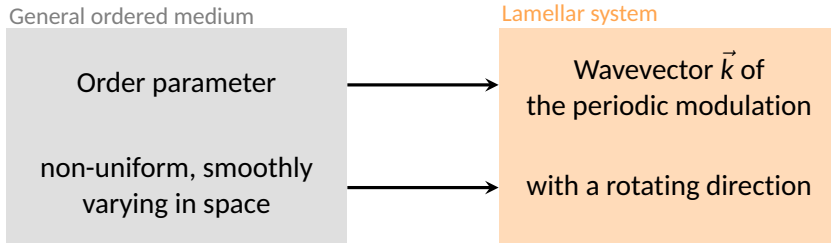
Topological defects in lamellar systems

General ordered medium

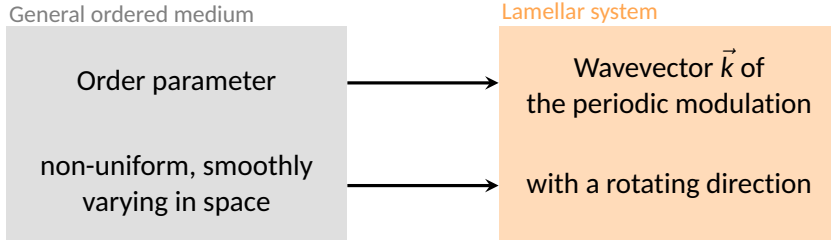
Order parameter

non-uniform, smoothly
varying in space

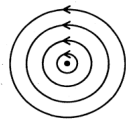
Topological defects in lamellar systems



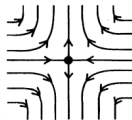
Topological defects in lamellar systems



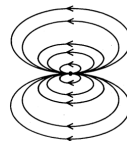
except at singular regions of lower dimensionality → topological defects



disclination
winding number = 1

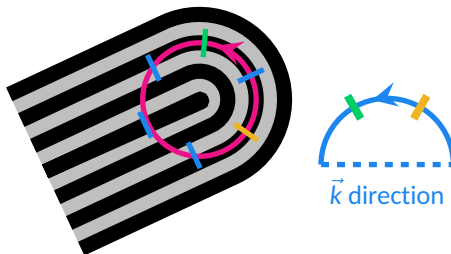
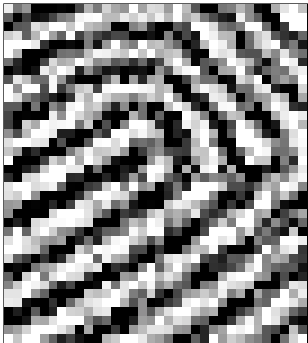


disclination
winding number = -1



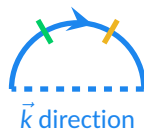
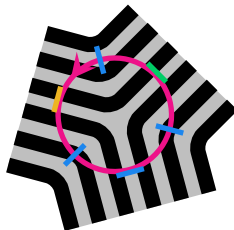
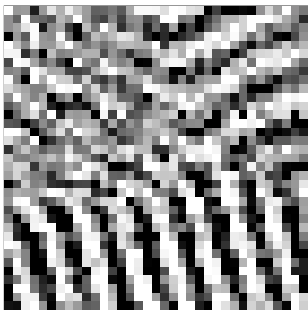
disclination
winding number = 2

$+\pi$ -disclination



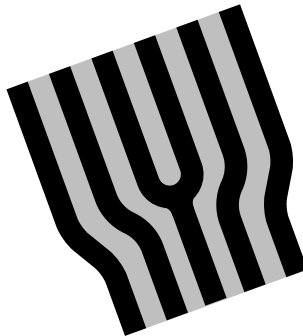
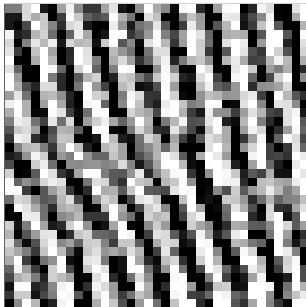
winding number $+1/2$

$-\pi$ -disclination



winding number $-1/2$

Edge dislocation

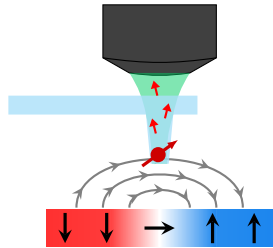


Combination of
 $+\pi$ - and $-\pi$ -disclinations

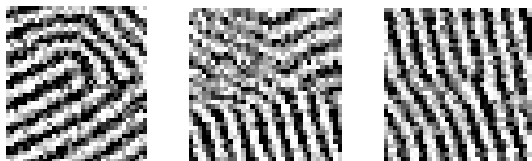
winding number 0

Summary

NV center magnetometry



Topological defects in multiferroic BiFeO₃



- highly sensitive
- nanoscale
- quantitative
- non-perturbative

Towards electric control?

A. Finco et al. *Phys. Rev. Lett.* 128 (2022), 187201

The team S2QT in Montpellier



We are looking for students and postdocs!